

# Facile fabrication of $\text{TiO}_2@\text{TiO}_2$ transparent free-standing film for photocatalysis

Shanmei Zhang<sup>1</sup>, Yue Hu<sup>2</sup>, Luyang Hu<sup>2</sup> ✉, Yumin Zhang<sup>3</sup>, Yufeng Zhou<sup>3</sup>, Benxia Li<sup>4</sup>

<sup>1</sup>School of Mathematic and Big Data, Anhui University of Science and Technology, Huainan 232001, People's Republic of China

<sup>2</sup>School of Materials Science and Engineering, Anhui University of Science and Technology, Huainan 232001, People's Republic of China

<sup>3</sup>Center for Composite Materials and Structure, Harbin Institute of Technology, Harbin 150001, People's Republic of China

<sup>4</sup>Department of Chemistry, College of Science, Zhejiang Sci-Tech University, Hangzhou 310018, People's Republic of China

✉ E-mail: huluhuyang@aliyun.com

Published in Micro & Nano Letters; Received on 30th April 2018; Revised on 5th August 2018; Accepted on 21st September 2018

A transparent titanium dioxide ( $\text{TiO}_2$ )@ $\text{TiO}_2$  film with free-standing structure was synthesised by employing a cellulose paper as the template. By one-step hydrothermal method and subsequent thermal annealing, the fibre of cellulose paper was changed into porous  $\text{TiO}_2$  core layer. The flower-like micro/nanostructure  $\text{TiO}_2$  particle layer was intimately distributed on the porous  $\text{TiO}_2$  core layer. The average diameter of the  $\text{TiO}_2@\text{TiO}_2$  fibre for the film was 11  $\mu\text{m}$ . The size of spherical granular  $\text{TiO}_2$  on the fibre surface was around  $330 \pm 130$  nm. It was noted that the microtopography of fibre surface could be adjusted by tuning the hydrothermal temperature. The scanning electron microscopy and  $\text{N}_2$  adsorption-desorption measurement results indicated that the prepared film possessed a large mass of mesopores and macropores. On the basis of the special microstructure, the  $\text{TiO}_2@\text{TiO}_2$  film exhibited high photocatalytic activity for methylene blue under ultraviolet irradiation. This work might provide a new insight for preparation of transparent photocatalytic film toward water purification.

**1. Introduction:** Titanium dioxide ( $\text{TiO}_2$ ), as an excellent semiconductor photocatalyst, has been widely applied in environmental treatment [1]. However, the application of powdered  $\text{TiO}_2$  for wastewater treatment has a drawback of post-separation from solution system after photocatalytic reaction [2]. An alternative approach to solve this problem is to form a  $\text{TiO}_2$  film on certain substrate such as glass [1, 3–5], carbon fibre [6], Ti foil [7], polycarbonate slide [8] and stainless steel [9]. The main synthesis methods for  $\text{TiO}_2$  film including chemical vapour deposition [3], dip coating [1, 4, 8], hydrothermal reaction [5–7] and spin coating [9]. It is noted that most of the carriers only play a supporting role, which do not exhibit significant benefit to improve the photocatalytic performance. Therefore, the preparation method of free-standing  $\text{TiO}_2$  film is developed.

Anodic oxidation of Ti foil as a major preparation technique for free-standing  $\text{TiO}_2$  film attracts tremendous interest because the obtained film has well-aligned  $\text{TiO}_2$  nanotube arrays, which exhibit a larger surface area, vectorial charge transfer and high photograph and chemical stability [10–12]. However, the free-standing film separated from the original substrate may cause the 1D nanostructure shrinkage to form an entangled mess or cracked structure [13]. The electrospinning method as a powerful and versatile technique has been applied to various materials. Combining electrospinning and subsequent hydrothermal treatment, free-standing  $\text{TiO}_2$  films with relatively large-scale and controllable microstructure can also be obtained [14]. Although the hydrothermal process usually is used to synthesise 1D structure in the nanoscale or microscale [14], 3D free-standing  $\text{TiO}_2$  nanofibre membranes with high photocatalytic activity are fabricated by reduced graphene oxide or carbon nanotube as linkers between the nanofibres [15, 16]. Recently, the one-step hydrothermal route to prepare transparent free-standing  $\text{TiO}_2$  film is also reported by dynamically changing the concentrations of  $\text{H}^+$ ,  $\text{Ti}^{3+}$  and  $\text{Cl}^-$  [13]. The film is comprised of 1D rutile/anatase  $\text{TiO}_2$  nanorod arrays, but it does not exhibit high photocatalytic performance.

In this Letter, a thin lint-free cellulose paper with uniform cellulose fibre is used as template. By one-step hydrothermal process and subsequent heat annealing under air atmosphere, a  $\text{TiO}_2@\text{TiO}_2$  transparent free-standing film is obtained. The synthesised

process is simple and the microstructure of film can be easily controlled by adjusting hydrothermal temperature. The functional material of novel structure may find use in photocatalytic application.

**2. Experiments:** In our experiment, the cellulose- $\text{TiO}_2@\text{TiO}_2$  film was first prepared as previously described [17]. Briefly, 1 mmol potassium titanium oxalate (PTO) was dissolved in 20 ml of mixed solution with diethylene glycol (DEG) and water ( $V:V=1:1$ ) by constant intense stirring. The solution was then transferred into a teflon-lined stainless autoclave. A piece of pretreated cellulose paper was placed in the autoclave and kept in an oven at 150–180°C for 6 h. After the autoclave cooled down to room temperature, the product was thoroughly washed with deionised water and dried at 60°C in vacuum over. To obtain the  $\text{TiO}_2@\text{TiO}_2$  transparent free-standing film, an as-synthesised cellulose- $\text{TiO}_2@\text{TiO}_2$  film was subsequently calcined at 500°C under air atmosphere for 2 h.

X-ray diffraction (XRD) pattern was recorded on an X-ray diffractometer with Cu  $K\alpha$  radiation (XRD 6000). The structural information of the product was obtained by scanning electron microscope (XL30 ESEM TMP) and gas adsorption measurement (ASAP 2020).

Photocatalytic activity test for methylene blue (MB) removal was performed at room temperature. The sample (1.2 cm  $\times$  3.0 cm, ~5 mg) was immersed in 10 ml MB solution (10 mg/ml) for 2 h in the dark, and then illuminated by two 8 W black-light tubes with a spectral peak centred at 365 nm. The absorbance of MB was measured at regular intervals of 20 min by ultraviolet (UV)-visible spectroscopy (UV-2600).

**3. Results and discussion:** Fig. 1a shows photographs of cellulose paper, cellulose- $\text{TiO}_2@\text{TiO}_2$  and  $\text{TiO}_2@\text{TiO}_2$  films. The white transparent cellulose paper transforms into a cellulose- $\text{TiO}_2@\text{TiO}_2$  film after hydrothermal treatment. The film exhibits a transparent structure. When the cellulose- $\text{TiO}_2@\text{TiO}_2$  film is calcined in air, transparent  $\text{TiO}_2@\text{TiO}_2$  film is obtained. No obvious cracks and wrinkles in the as-prepared film are observed. The XRD patterns of the three samples are presented in Fig. 1b.

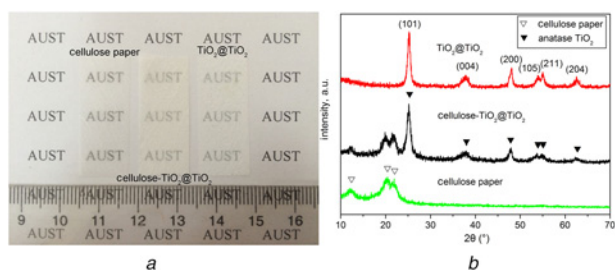


**Fig. 1** Photographs and XRD patterns of the samples  
a Photographs  
b XRD patterns

As shown in Fig. 1b, the well-defined peaks at  $25.3^\circ$ ,  $37.8^\circ$ ,  $48.0^\circ$ ,  $53.9^\circ$ ,  $55.1^\circ$  and  $62.7^\circ$  which correspond, respectively, to the (101), (004), (200), (105), (211) and (204) crystallographic planes of anatase  $\text{TiO}_2$  (JCPDS Card No. 84-1285) appear on the cellulose- $\text{TiO}_2$ @ $\text{TiO}_2$  film, except for three diffraction signals of cellulose paper. All diffraction peaks of anatase  $\text{TiO}_2$  on the cellulose- $\text{TiO}_2$ @ $\text{TiO}_2$  film are preserved on the  $\text{TiO}_2$ @ $\text{TiO}_2$  film after calcination.

Fig. 2 shows the SEM images of the  $\text{TiO}_2$ @ $\text{TiO}_2$  film. The film inherits the uniform fibre and 3D reticulate structure of cellulose paper [17]. The average diameter of fibre in film is  $11\ \mu\text{m}$ . The spherical granular  $\text{TiO}_2$  distributed on the fibre surface can be clearly observed (Figs. 2b and c). On the magnified micrograph, the  $\text{TiO}_2$  spheres with a diameter around  $330 \pm 130\ \text{nm}$  which are self-assembled by the  $\text{TiO}_2$  nanorods present flower-like hierarchical micro/nanostructure (Fig. 2d). In the cross-section of fibre, a microtopography different from that of surface  $\text{TiO}_2$  is exhibited

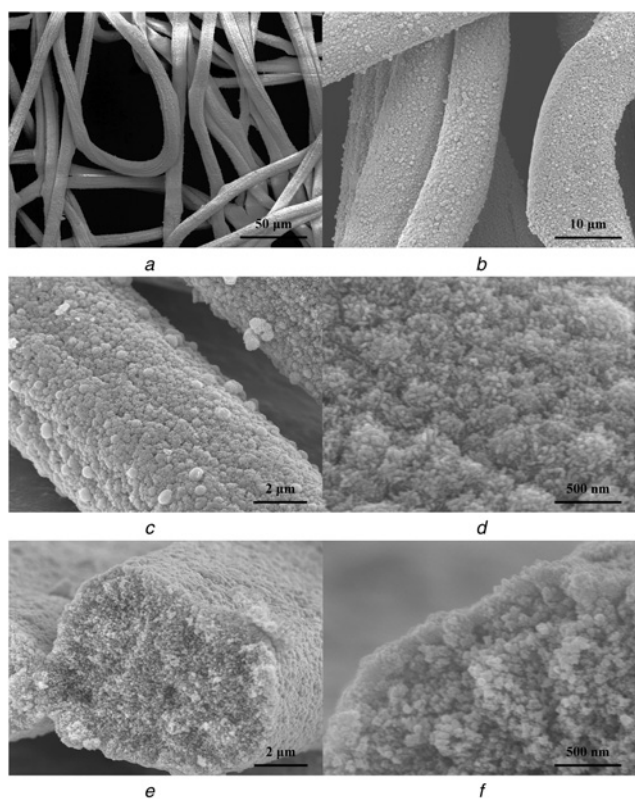


**Fig. 2** SEM images of the  $\text{TiO}_2$ @ $\text{TiO}_2$  film. The hydrothermal temperature is  $150^\circ\text{C}$   
a and b Fibre network  
c and d Fibre surface  
e and f Fibre cross-section

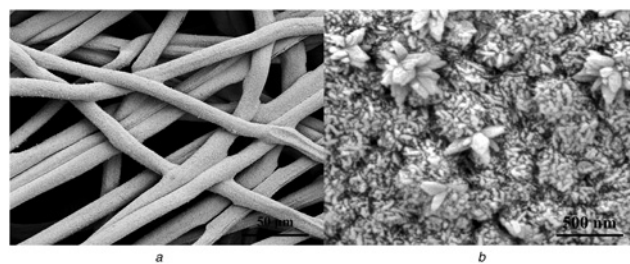


**Fig. 3** SEM images of the  $\text{TiO}_2$ @ $\text{TiO}_2$  film. The hydrothermal temperature is  $180^\circ\text{C}$   
a Fibre network  
b Fibre surface

in the inside of fibre (Figs. 2e and f). The  $\text{TiO}_2$  nanoparticles connect to each other to form the porous core layer. This is probably derived from the calcination of in situ mineralisation of cellulose fibre, because cellulose fibre contains a large number of nanopores and hydroxyl groups [18], which supply high-affinity sites for in situ synthesis of  $\text{TiO}_2$  nanoparticles. In fact, the microstructure of  $\text{TiO}_2$ @ $\text{TiO}_2$  fibre surface can be easily adjusted by varying hydrothermal temperature, and internal microstructure of fibre has no remarkable changes. Fig. 3 shows the SEM photographs of the  $\text{TiO}_2$ @ $\text{TiO}_2$  film prepared at  $180^\circ\text{C}$ . When the temperature is changed, there is no obvious influence on reticulate structure of the film, but some  $\text{TiO}_2$  nanosheets with about  $18\ \text{nm}$  in thickness occur on  $\text{TiO}_2$  submicrospheres of the fibre surface.

To investigate the pore characteristic of the  $\text{TiO}_2$ @ $\text{TiO}_2$  film, the nitrogen adsorption-desorption measurement is performed at  $77\ \text{K}$  (Fig. 4). As shown in the isotherm, the film presents a typical type-IV curve. A H3 type hysteresis loop can be observed at a relative pressure range of  $0.4$ – $1.0$ , suggesting the existence of slit-shaped pores. In addition, almost vertical tail occurs at relative pressure near  $1.0$ , which indicates that a fraction of macropores is also included in the film (Figs. 2d and f). The pore-size distributions calculated from the adsorption branch of the isotherm is plotted in the inset of Fig. 4. The mesopore size is mainly distributed in the range  $2$ – $10\ \text{nm}$ . According to the Brunauer-Emmett-Teller and Barrett-Joyner-Halenda methods, the film with a specific surface area of  $86.5\ \text{m}^2/\text{g}$  and pore volume of  $0.31\ \text{cm}^3/\text{g}$  is obtained.

To evaluate the performance of the  $\text{TiO}_2$ @ $\text{TiO}_2$  film for photocatalytic removal of organic dye from water, the photodegradations of MB in water is chosen as the model reaction (Fig. 5). In the experiment, photodegradations of MB in the absence of any catalyst and in the presence of P25 are also measured. Before the UV light irradiation, the photocatalyst is immersed in the MB solution for  $2\ \text{h}$

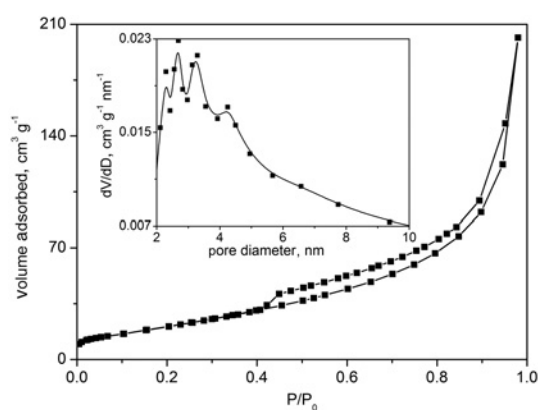


**Fig. 4**  $\text{N}_2$  adsorption-desorption isotherm and pore-size distribution plot of the  $\text{TiO}_2$ @ $\text{TiO}_2$  film

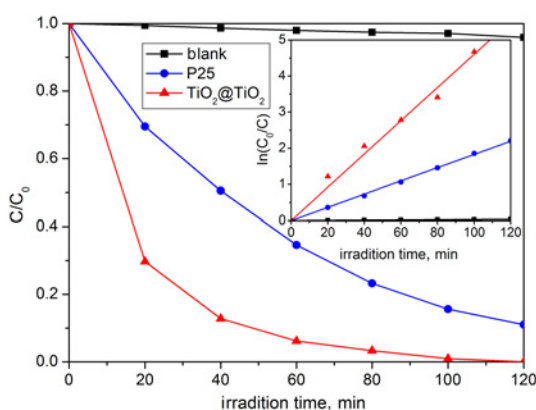


**Fig. 5** Degradation profiles of MB under UV light irradiation and kinetic linear simulation curves

in the dark to establish an adsorption–desorption equilibrium. The amounts of dye adsorption at equilibrium for the  $\text{TiO}_2@\text{TiO}_2$  film and P25 are 8.5 and 5.3 mg/g, respectively. After UV irradiation for 2 h, all dye molecules are degraded by the  $\text{TiO}_2@\text{TiO}_2$  film, and 96 and 11% MB still remain in the solution for the blank and comparison test (Fig. 5). According to the description of a pseudo-first-order kinetic model [ $\ln(C_0/C) = kt$ ], the kinetic constants  $k$  for the  $\text{TiO}_2@\text{TiO}_2$  film and P25 are 0.046 and 0.018/min, respectively. The enhanced photocatalytic activity may be attributed to the special microstructure and high specific surface of the  $\text{TiO}_2@\text{TiO}_2$  film, which increase absorptions of dye and active free radicals ( $\text{O}_2^-$  and  $\text{OH}$ ) of  $\text{TiO}_2$  surface under UV light illumination.

**4. Conclusion:** In summary, we have synthesised a  $\text{TiO}_2@\text{TiO}_2$  free-standing film by one-step hydrothermal process and subsequent calcination in air. The obtained film possessed the uniform fibre and a 3D reticulate structure. The spherical granular  $\text{TiO}_2$  with flower-like hierarchical micro/nanostructure on the fibre surface was observed. The  $\text{TiO}_2$  nanoparticles which came from the thermal annealing of in situ mineralisation of cellulose fibre connect to each other to form the porous core layer. By controlling hydrothermal temperature, the microstructure of surface  $\text{TiO}_2$  could be easily adjusted. In addition, the prepared  $\text{TiO}_2@\text{TiO}_2$  film shows obvious mesopores and macropores. Combining with adsorption and photodegradation of dye molecules, the  $\text{TiO}_2@\text{TiO}_2$  film exhibited high removal activity for MB.

**5. Acknowledgments:** This work was supported by the National Natural Science Foundation of China (grant nos. 51208003 and 21471004), young and middle-aged academic backbone training project and the introduced doctor's start-up fund from the Anhui University of Science and Technology and Major State Basic Research Program (grant no. 2014CB46505).

## 6 References

- [1] Du J., Lai X., Yang N., *ET AL.*: 'Hierarchically ordered macro-mesoporous  $\text{TiO}_2$ -graphene composite films: improved mass transfer, reduced charge recombination, and their enhanced photocatalytic activities', *ACS Nano*, 2011, **5**, (1), pp. 590–596
- [2] Yao Y., Ochiai T., Ishiguro H., *ET AL.*: 'Antibacterial performance of a novel photocatalytic-coated cordierite foam for use in air cleaners', *Appl. Catal. B, Environ.*, 2011, **106**, (3–4), pp. 592–599
- [3] Sotelo-Vazquez C., Noor N., Kafizas A., *ET AL.*: 'Multifunctional P-doped  $\text{TiO}_2$  films: a new approach to self-cleaning, transparent conducting oxide materials', *Chem. Mater.*, 2015, **27**, (9), pp. 3234–3242
- [4] Kamegawa T., Suzuki N., Yamashita H.: 'Design of macroporous  $\text{TiO}_2$  thin film photocatalysts with enhanced photofunctional properties', *Energy Environ. Sci.*, 2011, **4**, (4), pp. 1411–1416
- [5] Zhao Z., Tan H., Zhao H., *ET AL.*: 'Orientated anatase  $\text{TiO}_2$  nanocrystal array thin films for self-cleaning coating', *Chem. Commun.*, 2013, **49**, (79), pp. 8958–8960
- [6] Liang P., Wei A., Zhang Y., *ET AL.*: 'Immobilisation of  $\text{TiO}_2$  films on activated carbon fibres by a hydrothermal method for photocatalytic degradation of toluene', *Micro Nano Lett.*, 2016, **11**, (9), pp. 539–544
- [7] Zheng Z., Chen J., Yoshida R., *ET AL.*: 'One-step synthesis of  $\text{TiO}_2$  nanorod arrays on Ti foil for supercapacitor application', *Nanotechnology*, 2014, **25**, (43), p. 435406
- [8] Fateh R., Ismail A.A., Dillert R., *ET AL.*: 'Highly active crystalline mesoporous  $\text{TiO}_2$  films coated onto polycarbonate substrates for self-cleaning applications', *J. Phys. Chem. C*, 2011, **115**, (21), pp. 10405–10411
- [9] Pan J., Lei Z., Lee W., *ET AL.*: 'Mesoporous  $\text{TiO}_2$  photocatalytic films on stainless steel for water decontamination', *Catal. Sci. Technol.*, 2012, **2**, (1), pp. 147–155
- [10] Lin C., Yu W., Lu Y., *ET AL.*: 'Fabrication of open-ended high aspect-ratio anodic  $\text{TiO}_2$  nanotube films for photocatalytic and photoelectrocatalytic applications', *Chem. Commun.*, 2008, **44**, (45), pp. 6031–6033
- [11] Ouyang H., Fei G., Zhang Y., *ET AL.*: 'Large scale free-standing open-ended  $\text{TiO}_2$  nanotube arrays: stress-induced self-detachment and in situ pore opening', *J. Mater. Chem. C*, 2013, **1**, (45), pp. 7498–7506
- [12] Cho I.S., Choi J., Zhang K., *ET AL.*: 'Highly efficient solar water splitting from transferred  $\text{TiO}_2$  nanotube arrays', *Nano Lett.*, 2015, **15**, (9), pp. 5709–5715
- [13] Kao L.C., Lin C.J., Dong C.L., *ET AL.*: 'Transparent free-standing film of 1D rutile/anatase  $\text{TiO}_2$  nanorod arrays by a one-step hydrothermal process', *Chem. Commun.*, 2015, **51**, (29), pp. 6361–6364
- [14] Sun C., Wang N., Zhou S., *ET AL.*: 'Preparation of self-supporting hierarchical nanostructured anatase/rutile composite  $\text{TiO}_2$  film', *Chem. Commun.*, 2008, **44**, (28), pp. 3293–3295
- [15] Zhu L., Gu L., Zhou Y., *ET AL.*: 'Direct production of a free-standing titanate and titania nanofiber membrane with selective permeability and cleaning performance', *J. Mater. Chem.*, 2011, **21**, (33), pp. 12503–12510
- [16] Zhu L., Zhou L., Li H., *ET AL.*: 'One-pot growth of free-standing CNTs/ $\text{TiO}_2$  nanofiber membrane for enhanced photocatalysis', *Mater. Lett.*, 2013, **95**, pp. 13–16
- [17] Hu L., Zhang Y., Zhang S., *ET AL.*: 'A transparent  $\text{TiO}_2$ -C/ $\text{TiO}_2$ -graphene free-standing film with enhanced visible light photocatalysis', *RSC Adv.*, 2016, **6**, (49), pp. 43098–43103
- [18] He J., Kunitake T., Nakao A.: 'Facile in situ synthesis of noble metal nanoparticles in porous cellulose fibers', *Chem. Mater.*, 2003, **15**, (23), pp. 4401–4406